

Preference of $np_{\pi}-np_{\pi}$ Bonding ($n = 3, 4$) over Purely σ -Bonded Species in M_4^{2+} ($M = S, Se$): Geometries, Bonding, and Energetics of Several M_4^{2+} Isomers^{†,‡}

Ingo Krossing and Jack Passmore*

University of New Brunswick, Chemistry Department, Fredericton, New Brunswick, E3B 6E2 Canada

Received January 6, 1999

The dimerization energies of $2M_2^+$ to give M_4^{2+} ($M = S, Se$) were calculated as input into thermodynamic Born–Fajans–Haber cycle calculations to determine the relative stabilities of salts of these mono- and dications in the solid state. Computed dimerization energies showed a strong dependence on the basis set and correlated method utilized. Coupled cluster calculations, compound methods or hybrid HF/DFT methods employing large basis sets [CCSD(T)/cc-pV5Z, CBS-Q or B3PW91/6-311+G(3df)//B3PW91/6-311+G*] had to be used and showed an average dimerization energy of 258 (199) kJ/mol for sulfur (selenium). Square planar M_4^{2+} ($M = S, Se$) was fully optimized (B3LYP, B3PW91), and the calculated vibrational spectra of M_4^{2+} were then compared to averaged experimental data to derive scaling factors. The structure, bonding, and energetics of seven starting geometries of the M_4^{2+} ($M = S, Se$) dication were computed (B3PW91), as well as AIM and NBO analyses of these species. The global minimum of the examined sulfur (selenium) species is the planar, 6π -aromatic D_{4h} symmetric square, which is 76 (106) and 155 (115) kJ/mol more stable than a D_{2h} symmetric $\pi^*-\pi^*$ -bonded rectangular (S_2^+)₂ [(Se₂⁺)₂] dimer and a classical, σ -bonded, butterfly-shaped isomer, respectively. This supports the thesis that the observed geometries of the homopolyatomic cations of groups 16 and 17 and related species maximize positive charge delocalization, resulting in thermodynamically stable $np_{\pi}-np_{\pi}$ ($n \geq 3$) and $\pi^*-\pi^*$ bonds. The formation of chain-like (Te₄²⁺)_n, polymeric Te₈⁴⁺, and square planar Te₄²⁺ is accounted for semiquantitatively. The published, experimental enthalpy of formation of gaseous S₄⁺ (1131 kJ/mol) was computationally shown to be due to a fragmentation of S₆ to give S₄⁺ and S₂, confirming earlier photoionization studies. An enthalpy of formation of 972 kJ/mol was then established for the gaseous S₄⁺ cation, 159 kJ/mol lower than the erroneously assigned published experimental value.

Introduction

The electronegative elements are usually associated with anion formation, e.g., Cl[−] and S^{2−}. However, over the last 30 years, a number of homopolyatomic cations of the elements of group 16 have been prepared as salts of very weakly basic, nonoxidizable anions. They were recently reviewed by J.P. in 1989¹ and by J. Beck in 1994 and 1997.² With the exception of O₂⁺, all the known salts containing homopolyatomic cations of group 16 are diamagnetic multicharged species: e.g., S_n²⁺, $n = 4, 8, 19$; Se_n²⁺, $n = 4, 8, 10, 17$; Te_n²⁺, $n = 4, 6, 7, 8, 10$; Te_n⁴⁺, $n = 6, 8.^{1,2} Although the existence of singly charged, colored sulfur homopolyatomic radical cations in solution at low concentration has been well established, including blue S₅⁺, and what is probably S₇⁺,³ no isolable salt of such a heavier chalcogen radical cation has been synthesized so far. In our efforts to understand the exclusive formation of diamagnetic$

dications, we are currently performing a series of thermodynamic lattice potential energy and Born–Fajans–Haber cycle calculations to model the solid-state behavior of the homopolyatomic chalcogen cations.⁴ An important input into these cycles is the accurate gas-phase dimerization energy of the respective species as obtained by ab initio calculations.

Square planar M_4^{2+} dications ($M = S, Se, Te$) have been known for some time,^{1,2} but recently two new “(Te^{0.5+})_n” cations, a Te₄²⁺ dimer (=Te₈⁴⁺) and a polymeric (Te₄²⁺)_n chain, were published by J. Beck et al.² (see Figure 1).

Similarly four isomers of the Te₈²⁺ dication are now established in the solid state, which is contrasted with the presence of only a single isomer for S₈²⁺ and Se₈²⁺.^{1,2} This raises the question of why a more diverse structural chemistry is found for the heavier tellurium cations. We account for the bonding in these new tellurium species on a qualitative/semiquantitative basis.

Theoretical calculations of the S₄²⁺ dication were reported as early as 1979 by Fukui and co-workers.⁵ They, as well as later groups,^{6–10} were able to reproduce computationally the

[†] Dedicated to Prof. Dr. Dr. h.c. mult. Heinrich Nöth on the occasion of his 70th birthday.

[‡] Part of this work was presented at the 1998 CIC Conference in Whistler, British Columbia, Canada, and the 12th European Symposium on Fluorine Chemistry in Berlin, Germany, 1998.

- (1) (a) Burford, N.; Passmore, J.; Sanders, J. C. P. In *From Atoms to Polymers, Isoelectronic Analogies*; Liebman, J. F., Greenburg, A., Eds.; VCH: New York, 1989; pp 53–108 and references therein. (b) Passmore, J.; Klapötke, T. M. *Acc. Chem. Res.* **1989**, *22*, 234. (c) Passmore, J. In *The Chemistry of Inorganic Ring Systems*; Stuedel, R., Ed.; Studies in Inorganic Chemistry, Vol 14; Elsevier: Amsterdam, 1992; Chapter 19, pp 373–406.
- (2) (a) Beck, J. *Angew. Chem., Int. Ed. Engl.* **1994**, *33*, 163. (b) Beck, J. *Coord. Chem. Rev.* **1997**, *163*, 55.
- (3) Burns, R. C.; Gillespie, R. J.; Sawyer, J. F. *Inorg. Chem.* **1980**, *19*, 1423.

- (4) Cameron, T. S.; Roobottom, H. K.; Dionne, I.; Passmore, J.; Jenkins, H. D. B. Submitted to *Inorg. Chem.*
- (5) Tanaka, K.; Yamabe, T.; Terama, H.; Fukui, K. *Inorg. Chem.* **1979**, *18*, 3591.
- (6) (a) Saethre, L. J.; Gropen, O. *Can. J. Chem.* **1992**, *70*, 348. (b) Gropen, O.; Saethre, L. J.; Wilsoff-Nielssen, E. In *Studies in Physical and Theoretical Chemistry*; Carbo, Ed.; Elsevier: Amsterdam, 1982; p 427.
- (7) Kao, J. J. *Mol. Struct.* **1980**, *63*, 293.
- (8) Tang, T. H.; Bader, R. F. W.; McDougall, P. J. *Inorg. Chem.* **1985**, *24*, 2047.
- (9) Skrezenek, F. L.; Harcourt, R. D. *Theor. Chim. Acta* **1985**, *67*, 271.

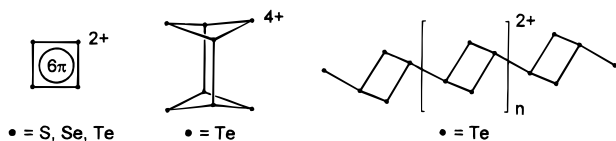


Figure 1. Experimentally determined structures of chalcogen cations in the +0.5 oxidation state.

square planar, D_{4h} symmetric geometry of S_4^{2+} found experimentally by Passmore et al.¹¹ The structure and π -bonding of the 6π -aromatic M_4^{2+} ($M = S, Se, Te$) was the focus of a 1992 ab initio study of Saethre and Gropen,⁶ preceded by earlier semiempirical calculations.^{5,12} Kutzelnigg¹³ reported in 1995 on the geometry and ^{77}Se NMR shift of Se_4^{2+} . The observed structures (X-ray in refs 1, 2, 14, and 15) are in good agreement with the calculated, but the NMR shifts are not even near the reported value. However, very recently T. Ziegler¹⁶ successfully modeled the NMR shift of Se_4^{2+} by pure DFT. The gas-phase dimerization reaction of $2S_2^+$ to give S_4^{2+} was examined for the first time in 1993 by F. Grein and M. Sannigrahi including an investigation of eight S_4^{2+} isomers. They found a dimerization energy of 443 kJ/mol (ROHF/6-31G*).¹⁷ From our investigations of the solid-state thermodynamics of this system,⁴ we realized that this dimerization energy must be too high. In the related $SN^+ + SNS^+ \rightarrow S_3N_2^{2+}$ system¹⁸ a similar gas-phase dimerization energy is reported (400 kJ/mol, HF/6-31G*). Dissolution of solid $S_3N_2(AsF_6)_2$ in liquid SO_2 and subsequent recording of the solution Raman spectrum reveal the exclusive presence of the monocations SN^+ and SNS^+ . This was also shown by inclusion of approximate solvation energies estimated by the Born equation.¹⁸ Using the calculated dimerization energy of 443 kJ/mol for the reaction of $2S_2^+$ to give S_4^{2+} and correcting for energies of solvation by the Born equation, SO_2 solutions of S_4^{2+} salts would be expected to contain S_2^+ monocations. However, dissolution of $S_4(AsF_6)_2$ in SO_2 in the presence of a large excess of AsF_5 (to increase the solubility and decrease the polarity of the solvent) followed by recording the solution Raman spectrum only showed bands attributable to the S_4^{2+} dication.^{4,11d,19} No evidence was found for the presence of S_2^+ , implying that the published gas-phase dimerization energy might be too high. We therefore undertook a new theoretical study of the M_2^+/M_4^{2+} ($M = S, Se$) system, and found dimerization energies varying widely at different levels of theory. Consequently we initiated a systematic study of correlation and basis set effects of these reactions and showed

that it is mandatory to use sophisticated methods and large basis sets to obtain thermochemically accurate values.²⁰ From the analysis of our recent results,²⁰ we concluded that one level of theory [e.g. CBS-Q or B3PW91/6-311+G(3df)//B3PW91/6-311+G*] described the system adequately at lowest computational cost. Using this method, we computed the structures of seven likely, low-energy M_4^{2+} isomers ($M = S, Se$) to identify the global minimum, to understand the exclusive formation of only one sulfur and selenium M_4^{2+} isomer, but three tellurium Te_4^{2+} isomers, and to verify that the D_{4h} isomer M_4^{2+} ($M = S, Se$), as characterized in the solid state by X-ray crystallography,^{11,14,15} is also the global minimum in the gas phase.

Computational Details

All calculations have been performed on a Pentium II personal computer (233–333 MHz, 128 MB of RAM) using the Gaussian94W²¹ suite of programs. Visualization of the optimized structures and critical points proceeded with the help of Dr. Holger Schwenk's RESVIEW program.²² Calculated vibrational frequencies have been visualized with the help of the program HyperChem.²³ All computed geometries were fully optimized at the given level of theory, followed by a frequency calculation to verify its nature as a stationary point on the hypersurface, and all are true minima unless stated otherwise. Zero point energies were included at various levels of theory, but these changed the energies by no more than 3–4 kJ/mol. Basis sets were used as implemented in Gaussian 94W.

Results and Discussion

Dimerization Energy for the Reaction of Two M_2^+ to Give M_4^{2+} . All reports on the solid-state geometry of M_4^{2+} ($M = S, Se, Te$)^{11,14,15} agree on a square planar D_{4h} symmetric structure for these dications. Therefore, we used this symmetry restriction for all calculations performed on the gas-phase dimerization energy. Various levels of theory and different basis sets gave dimerization energies for the $2S_2^+/S_4^{2+}$ system which range from 214 (MP2/cc-pVQZ) to 522 (CISSD/6-311G*) kJ/mol. Using the hybrid HF-DFT levels of theory (B3LYP and B3PW91), low values of the dimerization energy were obtained even with reasonably small basis sets [e.g., 254 kJ/mol with B3PW91/6-311G(2df)]. To understand the wide range of calculated dimerization energies, we initiated a systematic study of basis set and correlation effects on the ionization potential of S_2 and the gas-phase dimerization of M_2^+ to give M_4^{2+} ($M = S, Se$), which is published elsewhere.^{20,24} The problem was

- (10) Landwijk, G. V.; Janssen, R. A. J.; Buck, H. M. *J. Am. Chem. Soc.* **1990**, *112*, 4155.
 (11) (a) Passmore, J.; Sutherland, G. W.; White, P. S. *J. Chem. Soc., Chem. Commun.* **1980**, 330. (b) Passmore, J.; Sutherland, G. W.; White, P. S. *Inorg. Chem.* **1982**, *21*, 2717. (c) Passmore, J.; Sutherland, G. W.; Widdien, T. K.; White, P. S.; Wong, C. H. *Can. J. Chem.* **1985**, *63*, 1209. (d) Dionne, I. M.Sc. Thesis, University of New Brunswick, 1993. (e) Faggiani, R.; Gillespie, R. J.; Sawyer, J. F.; Vekris, J. E. *Acta Crystallogr.* **1989**, *C45*, 1847.
 (12) Foti, A. E.; Smith, V. H. Jr.; Salahub, D. R. *Chem. Phys. Lett.* **1978**, *57*, 33.
 (13) Bühl, M.; Thiel, W.; Fleischer, U.; Kutzelnigg, W. *J. Phys. Chem.* **1995**, *99*, 4000.
 (14) Brown, I. D.; Crump, D. B.; Gillespie, R. J. *Inorg. Chem.* **1971**, *10*, 2319.
 (15) Cardinal, G.; Gillespie, R. J.; Sawyer, J. F.; Vekris, J. E. *J. Chem. Soc., Dalton Trans.* **1982**, 765.
 (16) Ziegler, T. Presented at the 1998 CIC Conference in Whistler, British Columbia, Canada, Abstract No. 663.
 (17) Sannigrahi, M.; Grein, F. *Can. J. Chem.* **1994**, *72*, 298.
 (18) Brooks, W. V. F.; Cameron, T. S.; Parsons, S.; Passmore, J.; Schriver, M. J. *Inorg. Chem.* **1994**, *33*, 6230.
 (19) Dionne, I. Presented at the 1998 CIC Conference in Whistler, British Columbia, Canada, Abstract No. 591.

- (20) Jenkins, H. D. B.; Jitariu, L. C.; Crossing, I.; Passmore, J.; Suontamo, R. *J. Comput. Chem.*, in press.
 (21) Performed with the program Gaussian 94, Revision E.3: M. J. Frisch, G. W. Trucks, H. B. Schlegel, P. M. W. Gill, B. G. Johnson, M. A. Robb, J. R. Cheeseman, T. Keith, G. A. Petersson, J. A. Montgomery, K. Raghavachari, M. A. Al-Laham, V. G. Zakrzewski, J. V. Ortiz, J. B. Foresman, C. Y. Peng, P. Y. Ayala, W. Chen, M. W. Wong, J. L. Andres, E. S. Replogle, R. Gomperts, R. L. Martin, D. J. Fox, J. S. Binkley, D. J. Defrees, J. Baker, J. P. Stewart, M. Head-Gordon, C. Gonzalez, and J. A. Pople, Gaussian, Inc., Pittsburgh, PA, 1995.
 (22) RESVIEW, Version 2.21, by Dr. Holger Schwenk, University of Munich, 1998. E-mail: H.Schwenk@lrz.uni-muenchen.de.
 (23) HyperChem, V.3.0, Autodesk, 1993.
 (24) Even with the largest basis sets used [cc-pVQZ] neither MP2, MP3 nor MP4(SDQ) converged to a single value for the gas phase dimerisation energy of two S_2^+ to give S_4^{2+} which are still about 65 to 90 kJ/mol apart [MP2 vs. MP3 or MP4(SDQ)]. However, with increasing size of the basis set, the dimerisation energy decreased considerably from about 213 (MP2) to 303 kJ/mol [MP4(SDQ)]. The problem was finally solved by computing the dimerisation energy at the highly correlated CCSD(T) level and extrapolating the total energies obtained with the cc-pVDZ, cc-pVTZ, cc-pVQZ and cc-pV5Z basis sets to the complete basis set limit. Utilizing this procedure, adding the zero point energies and correcting the enthalpies to 298 K yielded the converged average gas phase dimerisation enthalpy of $2 S_2^+$ to give S_4^{2+} as 258 ± 9 kJ/mol.²⁰

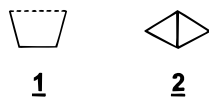


Figure 2. Starting geometries of **1** and **2**.

finally solved by employing the computationally very expensive CCSD(T)/cc-pV5Z level and also by the compound methods CBS-Q and Gaussian-2 which are reported to be the most accurate available within Gaussian 94²¹ and employ MP4 and QCISD(T) as the highest levels of theory. From these calculations we concluded an average gas-phase dimerization energy of two S₂⁺ to give S₄²⁺ of 258 ± 9 kJ/mol.²⁰ Initial results of the homologous selenium system only varied from 169 to 241 kJ/mol, indicating a less complex situation, and from our best calculations we concluded an average gas-phase dimerization energy of about 199 ± 20 kJ/mol.²⁵ In an analysis of all methods employed for both systems, we found that the hybrid HF-DFT level of theory B3PW91 reproduces energies and geometries of E₂, E₂⁺, and E₄²⁺ accurately at lowest computational cost. While B3PW91/6-311+G(3df)/B3PW91/6-311+G* is sufficient to describe the energetics of the sulfur species, B3PW91/6-311G(2df) gives the geometries closest to experiment of all methods employed.²⁰ All other correlated levels consistently overestimated the M–M bond lengths by 2–6 pm.

Independent Calculation of ΔH_{dim} and $\Delta H_{\text{f}}^{298}(\text{S}_4^{2+})$. To check our previously obtained value of 258 kJ/mol²⁰ in an independent calculation, the enthalpy of formation of S₄²⁺_(g) was needed to calculate the dimerization enthalpy of the reaction of 2S₂⁺_(g) → S₄²⁺_(g). Since this property is not available, one can calculate this value according to

$$\Delta H_{\text{f}}^{298}(\text{S}_4^{2+})_{(\text{g})} = \Delta H_{\text{f}}^{298}(\text{S}_4(\text{g})) + {}^{1+2}\text{IP}(\text{S}_4)$$

where $\Delta H_{\text{f}}^{298}(\text{S}_4(\text{g}))$ is the experimentally determined enthalpy of formation of neutral tetrasulfur and ${}^{1+2}\text{IP}(\text{S}_4)$ equals the sum of the calculated first and second ionization potentials of S₄. Our preceding calculations²⁰ lend high credibility to the B3PW91/6-311+G(3df)/B3PW91/6-311+G* level of theory, and therefore we calculated the structure and energy of neutral S₄ and S₄²⁺ with this method. Both species are closed shell systems, which further increases the accuracy of the calculation. The employed C_{2v} tetrasulfur geometry **1**²⁶ (see Figure 2) has been published twice²⁷ as the global minimum on the S₄ hypersurface [QCISD/TZ(2p)//HF/TZ(2p)], and the experimental vibronic absorption spectrum of neutral S₄ in solid argon is in agreement with this geometry being the ground state.²⁸ At the B3PW91/6-311+G(3df)/B3PW91/6-311+G* level of theory the combined first and second ionization potentials of neutral S₄ was computed as ${}^{1+2}\text{IP}(\text{S}_4) = 2172$ kJ/mol. $\Delta H_{\text{f}}(\text{S}_4)$ has been determined experimentally as 146 ± 8 kJ/mol,²⁹ giving $\Delta H_{\text{f}}(\text{S}_4^{2+})$ as

$$\Delta H_{\text{f}}^{298}(\text{S}_4^{2+})_{(\text{g})} = 2172 + 146(\pm 8) = 2318 \pm 8 \text{ kJ/mol}$$

Subtracting twice the experimental enthalpy of formation of S₂⁺ (1031 kJ/mol)²⁹ yields the enthalpy of the gas-phase dimerization of 2S₂⁺ to give S₄²⁺ as $\Delta H_{\text{dim}} = [2318(\pm 8) - (2 \times 1031)] = 256 \pm 8$ kJ/mol. This value is in excellent agreement with our previous conclusion²⁰ which assigned a value of 258 ± 9 kJ/mol.

Square Planar M₄²⁺ (M = S, Se) Geometries at the B3LYP and B3PW91 Levels of Theory. X-ray single-crystal structure determinations show the square planar, D_{4h} symmetric S₄²⁺ cation in various AsF₆⁻ and [(Sb₂F₄)(Sb₂F₅)(SbF₆)₅]²⁻ salts with S–S bond lengths that range from 1.975(5) to 2.015(2) Å.¹¹ The crystal structure of S₄(AsF₆)₂AsF₃^{11d} is well determined at low temperature and has been corrected for thermal motions. The S–S bond lengths in this cation are the most accurate available and average 2.011(3) Å. This compares well with the computed bond distances of the S₄²⁺ dication (D_{4h}) given in Table 1. They mirror experimentally observed values within a few picometers and range from 2.027 to 2.072 Å. All S–S distances computed by the hybrid HF-DFT methods are somewhat longer than the experimentally observed bond lengths. The larger the basis set, the shorter is d(S–S) in the optimized structures, e.g., B3LYP/6-311+G* (2.072 Å) vs B3LYP/AUG-cc-vPTZ (2.051 Å). Employing the B3PW91 level of theory together with the flexible 6-311G(2df) basis set gives the geometries closest to experiment [d(S–S) = 2.027 Å vs 2.011(3) Å (exptl)]. S₄²⁺ is found in a rather shallow potential, such that changing d(S–S) from 2.072 to 2.000 Å only increases the energy by 8 kJ/mol (B3LYP/6-311+G*). This explains the difficulties in mirroring the experimentally observed bond lengths exactly with all but the largest basis sets. The D_{4h} symmetric Se₄²⁺ dication is found in various salts in the solid state and exhibits an average Se–Se bond length of 2.284(4) Å³⁰ (not corrected for thermal motions, which adds approximately 1 pm). Computed Se–Se distances are given in Table 1. B3LYP and B3PW91 overestimate the Se–Se bond lengths by 2.5–5.8 pm. Similar to the sulfur system, the Perdew–Wang 1991 gradient-corrected correlation functional³¹ [d(Se–Se) = 2.309 and 2.319 Å] performs better than the older Lee–Yang–Parr functional³² [d(Se–Se) = 2.342 Å] and gives bond distances which are closer to the experimental values.

Vibrational Spectra. Raman spectra of a variety of salts of M₄²⁺ (M = S, Se) as well as solution spectra thereof have been obtained previously and are reported in the literature in detail.^{11d,33} Unequivocally assigned vibrational modes of S₄²⁺ have B_{2g} (606 ± 3 cm⁻¹), A_{1g} (587 ± 3 cm⁻¹), and B_{1g} (374 ± 7 cm⁻¹) symmetry. For Se₄²⁺ these modes exhibit A_{1g} (324 ± 3 cm⁻¹), E_u (303 ± 4 cm⁻¹), and B_{1g} (185 ± 3 cm⁻¹) symmetry. The B_{2g} mode is often not distinguished from the most intense symmetric A_{1g} mode.³³ Therefore, it is not included in the discussion. The given experimental frequencies cited are obtained as an average of the data of four different sources and include the maximum deviation observed. Used scaling factors are the average of the three factors obtained by scaling each frequency of each method individually for the best fit with experiment. Calculated harmonic frequencies without (with) scaling are summarized in Tables 2 (S) and 3 (Se) together with

(25) All methods converged to a single value within the basis sets employed, and we derived the gas-phase dimerization energy of the Se₄²⁺/2Se₂⁺ system from the average of the B3LYP, B3PW91, MP2, MP3, and MP4(SDQ) calculations employing the largest basis set.

(26) Optimized parameters S₄ in C_{2v} symmetry (UB3PW91/6-311+G*): d(S–S) = 1.921 Å (terminal) and 2.220 Å (central), ∠(S–S–S) = 104.1°, true minimum, Nimag = 0.

(27) (a) Zakrzewski, V. G.; Niessen, W. v. *Theor. Chim. Acta* **1994**, *88*, 75. (b) Quelch, G. E.; Schaefer, H. F.; Marsden, C. J. *J. Am. Chem. Soc.* **1990**, *112*, 8719.

(28) Hassanzadeh, P.; Andrews, L. *J. Phys. Chem.* **1992**, *96*, 6579.

(29) Wagman, D. D.; Evans, W. H.; Parker, V. B.; Schumm, R. H.; Halow, I.; Bailey, S. M.; Churney, K. L.; Nuttal, R. L. *J. Phys. Chem. Ref. Data* **1982**, *11*, Suppl. 2.

(30) Average of the Se₄(AlCl₄)₂ and Se₄(HS₂O₇)₂ structures in refs 14 and 15.

(31) Perdew, J. P.; Wang, Y. *Phys. Rev.* **1992**, *B 45*, 13244.

(32) Lee, C.; Yang, W.; Parr, R. G. *Phys. Rev.* **1988**, *37*, 785.

(33) Burns, R. C.; Gillespie, R. J. *Inorg. Chem.* **1982**, *21*, 3877 and references therein.

Table 1. Computed M–M Bond Lengths of the Square Planar M_4^{2+} Dications at the B3LYP and B3PW91 Levels of Theory (Å)

level of theory	S_4^{2+} (D_{4h}) $d(S-S)$	Se_4^{2+} (D_{4h}) $d(Se-Se)$
experiment	2.011(3) ^a	2.284(4) ^b
B3LYP/6-31G*	2.064	
B3LYP/6-311+G*	2.072	2.342
B3LYP/Aug-ccPVTZ	2.051	
B3PW91/6-311+G*	2.053	2.319
B3PW91/6-311G(2df)	2.027	2.309

^a Corrected for librational motion. ^b Not corrected for librational motion.

the respective M–M bond lengths and employed scaling factors. At all levels of theory, the experimental vibrational frequencies are reproduced reasonably well within $-18/+25$ cm^{-1} (scaled, S) or $-5/+12$ cm^{-1} (scaled, Se). The (arithmetic) average deviation from experiment is 12.1 cm^{-1} for S_4^{2+} and 4.6 cm^{-1} for the homologous selenium dication. Calculated S–S distances in S_4^{2+} vary from 2.027 to 2.072 Å depending on the method (Table 2). Consistently, the unscaled B_{2g} frequencies range from 570 to 625 cm^{-1} . The shorter $d(S-S)$, the higher the calculated unscaled vibrational frequency. Similarly, the calculated scaling factors for methods giving good geometries are closer to unity than those for less accurate levels of theory [e.g., 1.008 for B3PW91/6-311G(2df) and $d(S-S) = 2.027$ Å, but 1.088 for B3LYP/6-311+G* and $d(S-S) = 2.072$ Å].

The range of $d(Se-Se)$ in Table 3 is smaller (3.3 pm) than that found for the homologous sulfur system (5.5 pm), and Se–Se distances generally are about 30 pm longer than the S–S bond lengths. Therefore, a less pronounced dependence of the vibrational frequencies on the method is expected as observed in Table 3. Scaled calculated frequencies are found within 8 cm^{-1} (A_{1g}), 3 cm^{-1} (E_u), and 6 cm^{-1} (B_{1g}); they are in excellent agreement with the observed values.

A comparison of scaled and unscaled vibrational frequencies, employed scaling factors, and respective bond lengths in Tables 2 and 3 proves that one is not allowed to simply scale the calculated harmonic vibrational frequencies by the published normal or low-frequency factors (about 0.95 and 0.99 for B3PW91, 0.96 and 1.00 for B3LYP).³⁴ In these systems correlated methods combined with large basis sets are necessary to reproduce experimentally observed geometries [S, exptl 2.011(3) Å,^{11d} best computation, 2.027 Å, B3PW91/6-311G(2df); Se, exptl 2.284(4) Å,³⁰ best computation, 2.309 Å, B3PW91/6-311G(2df)]. Although scaling factors generally do not change much with different basis sets,³⁴ a strong dependence between basis set and scaling factor is expected here due to the variation of bond lengths with the size of the basis set. This holds for the two B3LYP optimizations employing the 6-311+G* basis set most markedly, where calculated harmonic vibrational frequencies were scaled by 1.088 (S) or 1.076 (Se) (compare to the published normal and low-frequency factors of 0.964 and 1.001 for the B3LYP/6-31G* level of theory).³⁴ However, the quality of the calculated, scaled vibrational frequencies is independent of the level of theory employed (see Tables 2 and 3). The description of the selenium system is easier than that of the sulfur system (e.g., the average deviation from experiment is lower, 4.6 vs 12.1 cm^{-1}), as found for the determination of the dimerization energies.²⁰

π -Bonding in Square Planar M_4^{2+} ($M = S, Se$). The description of the bonding in the square planar tetraelement dications M_4^{2+} ($M = S, Se$, and Te) is of special interest, since these are rare examples of experimentally characterized, ther-

modynamic stable compounds containing ($np-np$) π -bonds ($n \geq 3$) that are not protected by bulky groups.³⁵ Their 6π -aromatic character has been subject to an extensive ab initio study based on effective core potentials and inclusion of d-orbitals.⁶ Our investigations ($M = S$ and Se, B3LYP/6-311+G* and B3PW91/6-311+G* density) confirm Gropen's and Saethre's⁶ analysis. As expected from simple Hückel theory, four molecular orbitals of π -symmetry are formed, one bonding (A_{2u} , doubly occupied) orbital, two degenerate nonbonding (E_g , each doubly occupied) orbitals, and one antibonding (B_{2u} , unoccupied) orbital. An equivalent result is given by a natural bonding orbital analysis (NBO analysis, as implemented in Gaussian94W),³⁶ the 22 valence electrons are placed in four ns^2 lone pairs ($n = 3, 4$), four σ -MOs, two π -MOs, and two half-occupied π^* -MOs. The total ($\sigma + \pi$) formal bond order is $(4 + 2 - 1)/4 = 1.25$. This view is further supported by the calculated Wiberg (NAO) bond orders, which range from 1.243 (1.343) to 1.250 (1.390), verifying the presence of a π -contribution. An AIM analysis gives the expected 4 bond and one ring critical points.

Other M_4^{2+} ($M = S, Se$) Isomers. Analysis of the optimized M_4^{2+} ($M = S, Se$) geometries in Table 1 and our previous calculation of the dimerization energies²⁰ of $2M_2^{2+}$ to give M_4^{2+} reveal the particular strength of Becke's three-parameter exchange functional³⁷ combined with the 1991 Perdew–Wang correlational functional³¹ (B3PW91) in the description of homopolyatomic sulfur and selenium species. Therefore, this level of theory was selected to analyze the structure, bonding, and relative stabilities of other possible isomers of M_4^{2+} and to verify the exclusive use of the D_{4h} square planar structure for the computation of the gas-phase dimerization energies in our previous work.²⁰ Full optimizations (including frequency analysis) of seven isomers of M_4^{2+} ($M = S, Se$) have been performed at the B3PW91/6-311+G* level of theory to determine stationary points on the hypersurface, followed by single-point calculations at the B3PW91/6-311+G(3df) level of theory to obtain accurate total energies for the comparison of their relative stability. The two structures lowest in energy of each set (S and Se) have been fully reoptimized at the B3PW91/6-311G(2df) level of theory to verify the energetic ordering derived from the single-point calculations. Since the inclusion of the zero point correction only revealed energetic changes smaller than 4 kJ/mol, energies summarized here do not include this correction. Starting geometries have been a trapezoidal C_{2v} structure, **1** ($d(S-S)$ ($d(Se-Se)$) = 1.92 (2.20) and 2.19 (2.45) Å, $\angle(M-M-M) = 104^\circ$), a D_{2h} symmetric, planar bicycle, **2** ($d(S-S)$ ($d(Se-Se)$) = 2.05 (2.30) and 2.05 (2.30) Å, $\angle(M-M-M) = 60^\circ$), a butterfly-shaped C_{2v} bicycle, **3**, a D_{2h} rectangle, **4**, a planar D_{4h} square, **5**, a D_{3h} symmetric triangle, **6**, and a C_{2v} symmetric triangle with an exocyclic M atom, **7**. Some very unlikely structures (e.g., a M_4^{2+} tetrahedron and pyramid) have been omitted, since F. Grein et al.¹⁷ showed in 1994 for the sulfur system that their relative energies were much higher compared to those of the D_{2h} and D_{4h} isomers **4a** and **5a**. For the discussion of the bonding situation in the computed structures natural bonding orbital analysis (NBO analysis)³⁶ and Bader's atoms in molecules method (AIM method)³⁸ as implemented in Gaussian94W have been performed employing the B3PW91/6-311+G* electron density.

(35) See for example: *Multiply Bonded Main Group Metals and Metalloids*; West, R., Stone, F. G. A., Eds.; Academic Press: New York, 1996.

(36) Reed, A. E.; Curtiss, L. A.; Weinhold, F. *Chem. Rev.* **1988**, *88*, 899 and references therein.

(37) Becke, A. D. *J. Chem. Phys.* **1993**, *98*, 5648.

(38) Bader, R. F. W. *Acc. Chem. Res.* **1985**, *18*, 9.

(34) Scott, A. P.; Radom, L. *J. Phys. Chem.* **1996**, *100*, 16502.

Table 2. Experimental and Calculated Principal Vibrational Modes of S_4^{2+}

level of theory	scaling factor	B_{2g} (cm^{-1})	A_{1g} (cm^{-1})	B_{1g} (cm^{-1})	$d(S-S)$ (\AA)
experiment (av)		606 ± 3	587 ± 3	374 ± 7	2.011(3)
B3LYP/6-311+G*	1.088	570 (619)	523 (569)	343 (373)	2.072
B3LYP/6-31G*	1.063	587 (625)	536 (570)	352 (374)	2.064
B3PW91/6-311+G*	1.064	593 (631)	544 (579)	343 (364)	2.053
B3LYP/Aug-cc-pVTZ	1.045	595 (622)	552 (577)	355 (371)	2.051
B3PW91/6-311G(2df)	1.008	625 (631)	583 (588)	356 (359)	2.027

Table 3. Experimental and Calculated Principal Vibrational Modes of Se_4^{2+}

level of theory	scaling factor	A_{1g} (cm^{-1})	E_u (cm^{-1})	B_{1g} (cm^{-1})	$d(Se-Se)$ (\AA)
experiment (av)		324 ± 3	303 ± 4	185 ± 3	2.284(4)
B3LYP/6-311+G*	1.076	305 (328)	278 (299)	173 (186)	2.342
B3PW91/6-311+G*	1.011	332 (336)	296 (299)	179 (181)	2.319
B3PW91/6-311G(2df)	1.041	317 (330)	290 (302)	173 (180)	2.309

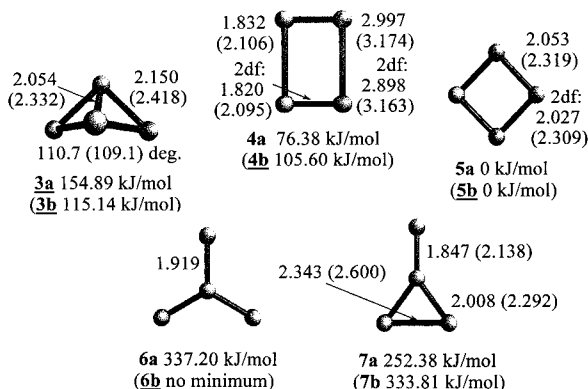


Figure 3. B3PW91/6-311+G* optimized structures and relative energies of the tetrasulfur (tetraselenium) dications **3a–7a** (**3b–5b**, **7b**). 2df precedes the bond distances obtained by B3PW91/6-311G-(2df) optimizations of the two most favorable M_4^{2+} ($M = S, Se$) isomers.

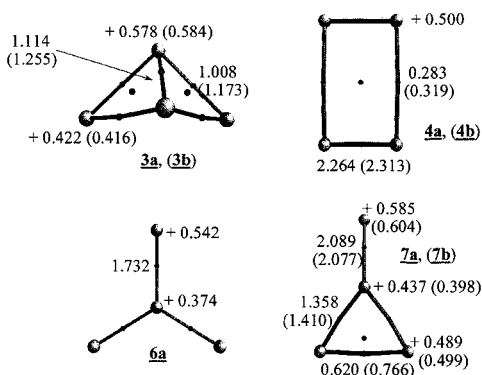


Figure 4. B3PW91/6-311+G* natural charges, NAO bond orders,³⁶ and bond and ring critical points³⁸ of the tetrasulfur (tetraselenium) dications **3a–7a** (**3b–5b**, **7b**).

Sulfur Geometries 1a–7a. Although isomer **1a** (Figure 2) is reported to be the global minimum of the neutral S_4 species [QCISD/TZ(2p)//HF/TZ(2p)],²⁷ it is not a minimum for S_4^{2+} and collapses to the D_{2h} rectangular structure **4a**. The planar D_{2h} bicycle **2a** (Figure 2) is not a minimum either and collapses to the D_{4h} square planar geometry **5a**. **3a–7a** are all true minima with no imaginary frequencies. Their optimized structures and relative energies are summarized in Figure 3, and their natural charges, NAO bond orders (=bo),³⁴ bond paths, and bond and ring critical points³⁸ are depicted in Figure 4.

Square Planar (5a) and Rectangular S_4^{2+} (4a). As in the solid state, the D_{4h} isomer **5a** is the global minimum in the gas phase, about 76 kJ/mol more favorable than the second best isomer **4a** (D_{2h}). The inclusion of polarizing f functions is

necessary and increases the relative stability of the square planar S_4^{2+} dication **5a** versus **4a** by about 50 kJ/mol compared to the results with the 6-311+G* basis set. The reoptimization of these two isomers with the larger 6-311G(2df) basis set gives the best square planar geometry obtained so far (2.027 Å vs 2.011(3) Å exptl^{11d}), but no further energetic changes (79 kJ/mol more favorable than **4a**). In the $\pi^*-\pi^*$ -bonded D_{2h} structure, the long S–S bond (bo 0.283) shrinks considerably by 0.1 Å from 2.997 to 2.898 Å when optimized with the larger basis set. This is consistent with a weak $\pi^*-\pi^*$ S–S bond¹ in **4a**, where small energetic changes have profound effects on the geometry. In contrast, the short bond (bo 2.264) shrank just by 1.2 pm. The expected bond critical points are found in the center between all bonded atoms, and a ring critical point is located in the center of the structure. An NBO analysis places the 22 valence electrons of the D_{2h} rectangle **4a** in four $3s^2$ lone pairs, two σ -MOs, four π -MOs, and two half-occupied π^* -MOs. It is best described as a weakly $\pi^*-\pi^*$ -bonded^{1a} rectangular (S_2^+)₂ dimer, 332 kJ/mol less stable than 2 equiv of gaseous S_2^+ [B3PW91/6-311+G(3df)//B3PW91/6-311+G*].

Butterfly (3a) and SO_3 -Like S_4^{2+} (6a). The C_{2v} and D_{3h} structures **3a** and **6a** are by 155 or 337 kJ/mol less stable than the D_{4h} isomer and are therefore not important in the gas-phase dimerization reaction. Their structures can be understood in the sense of more localized charges residing on the bridgehead S atoms in the C_{2v} structure **3a** or a dicationic trithio SO_3 -like derivative, **6a** (D_{3h}). **3a** is the classical all- σ -bonded alternative (bo 1.114 and 1.008) compared to the other structures which possess at least one formal π -bond and resembles the structure of the isoelectronic S_2P_2 ($S^+ \equiv P$), in agreement with calculated bond and ring critical points in Figure 4). The NBO analysis places the 22 valence electrons in four $3s^2$ and two $3p^2$ lone pairs (bridgehead sulfur atoms contain only $3s^2$ lone pairs), and the five σ bonds are represented by one σ -MO for the central cross ring bond and four σ -MOs for the remaining bonds. This all- σ -bonded isomer is 79 kJ/mol less stable than even the highly π -bonded (S_2^+)₂ isomer **4a**. However, the calculated natural charges in **3a** are delocalized [bridgehead, +0.578; bridging atom, +0.422]. This is achieved by a $3p^2 \rightarrow 3\sigma^*$ interaction which transfers electron density from the occupied $3p^2$ lone pairs of the dicoordinated sulfur atoms into the empty, vicinal $3\sigma^*$ orbital, shown in Figure 5.

The four equivalent $3p^2 \rightarrow 3\sigma^*$ interactions lower the total energy by about 93 kJ/mol and transfer in total about 0.21 of an electron into the $3\sigma^*$ orbitals (NBO analysis). Thus, even in this formally all- σ -bonded isomer there is some π bonding which leads to positive charge delocalization. **6a** contains three very short S–S bonds (1.919 Å) and comparable natural charges on all atoms (0.374 and 3×0.545), indicating delocalized charges

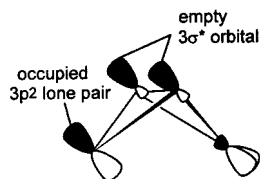


Figure 5. $3p^2 \rightarrow 3\sigma^*$ bonding in the butterfly-shaped S_4^{2+} isomer **3a**.

and the presence of partial double bonds [e.g., compare to $d(S=S)$ in S_2 , exptl 1.889 Å, calcd 1.914 Å (B3PW91/6-311+G*)]. Removal of 2 electrons from the highest occupied orbitals in the neutral D_{3h} S_4 species leads to a total of two $p\pi-p\pi$ bonds. Delocalization gives a formal ($\sigma + \pi$) bond order of $(3 + 2)/3 = 1.667$, which is in good agreement with the calculated NAO bond order of 1.732. Bond critical points are found as expected (see Figure 4), and the absence of ring points indicates that the terminal sulfur atoms are not interacting. However, the NBO analysis shows that 14 of the 22 valence electrons reside in three $3s^2$ lone pairs, three σ -MOs, and one π -MO. The remaining 8 electrons are delocalized over nine MOs of different symmetry, six of which differ less than 0.1 eV in relative energy. A total of 0.48 electron is found in the three σ^* -MOs about 0.3 eV higher in energy. Positive charge delocalization presumably is the driving force behind these interactions.

S_4^{2+} as a Triangle with an Exocyclic S Atom (7a). The structure of **7a** is 252 kJ/mol less stable than the D_{4h} isomer **5a** and thus not important for the gas-phase dimerization. A zeroth-order description of **7a** is provided by replacing the central, formally doubly charged sulfur atom by the isoelectronic silicon atom ($S^{2+} \equiv Si$). Its short exocyclic bond has a calculated NAO bond order of 2.089 [$d(S-S) = 1.847$ Å, compared to S_2^+ , calcd 1.831 Å (B3PW91/6-311+G*) with a formal bo of 2.5], the two short distances in the ring have a NAO bond order of 1.358 [$d(S-S) = 2.008$ Å, compared to S_4^{2+} (D_{4h}), calcd 2.053 Å (B3PW91/6-311+G*) with a formal bond order of 1.25], and the long bond has a NAO bond order of 0.620 with a corresponding very long S-S distance of 2.343 Å. According to the NBO analysis, this long bond is a pure $p\pi-p\pi$ bond. The corresponding antibonding π^* -MO is occupied by 0.51 electron, diminishing the bond order from 1 to the calculated 0.620. The $3p^2$ lone pairs at the two dicoordinated sulfur atoms are only occupied by 1.72 electron and form additional $p\pi-p\pi$ bonds to the central tricoordinated sulfur atom, thus increasing the bond order from 1 to the calculated 1.358. The exocyclic S atom is doubly bonded by a σ -bond and a π -bond as confirmed by the NAO bond order of 2.089. The positions of calculated bond critical points and the ring point in Figure 4 agree with this picture. As expected from the fractional occupation of the 6 electrons highest in energy distributed over seven molecular orbitals, the calculated natural charges are spread nearly evenly among the sulfur atoms (exo S, +0.585; central S, +0.398; 2S, +0.489).

Se_4^{2+} Geometries 1b–7b. The Se_4^{2+} hypersurface is very similar to that of the homologous sulfur system. Accordingly, **1b** and **2b** (Figure 2) are not minima and collapse to the respective **4b** and **5b** geometries. Additionally, after lowering the symmetry restraints to C_{2v} , the D_{3h} symmetric triangle **6b** optimizes to the triangular structure with an exocyclic Se atom, **7b**. **3b–5b** and **7b** are true minima on the hypersurface. Their geometries, energetics, and bonding are summarized in Figures 3 and 4. The description of their structures is similar to that of the sulfur system (see above), and calculated bond and ring critical points are found at similar positions. Conclusions drawn from the sulfur isomers hold for the selenium case as well. The

Table 4. Experimental Heats of Formation and Adiabatic Ionization Potentials of Neutral S_n ($n = 2-7$) and Heats of Formation of Gaseous S_n^+ ($n = 2-7$) (kJ/mol)²⁹

property	S_2	S_3	S_4	S_5	S_6	S_7
$\Delta H_f(S_{n(g)})_{\text{exptl}}$	129 ± 1	142 ± 8	146 ± 8	109 ± 8	102 ± 8	114 ± 8
IP_{exptl}	908 ± 1	934 ± 3	989 ± 29	830 ± 5	868 ± 3	837 ± 3
			calcd 826			
$\Delta H_f(S_n^+_{(g)})_{\text{exptl}}$	1031	1076	1131	939	971	951
			calcd 972			

global minimum is represented by the D_{4h} symmetric square **5b**, 106 kJ/mol more stable than the D_{2h} rectangle **4b**, which in turn justifies the exclusive use of the D_{4h} isomer **5b** in the determination of the gas-phase dimerization energy.²⁰ The reoptimization at the B3PW91/6-311G(2df) level of theory gives the best geometry obtained with correlated methods so far (2.309 Å, exptl 2.284(4) Å³⁰), but reveals no changes in the energetic ordering. Unlike in the sulfur D_{2h} structure **4a**, the use of the large 6-311G(2df) basis set hardly changes the length of the long ($\pi^*-\pi^*$) Se-Se bond¹ (bo 0.319) in **4b** (1.1 pm vs 9.9 pm in **4a**). Thus, the selenium system is less difficult to describe computationally than the homologous tetrasulfur dications. The short bond (bo 2.313) is highly π -bonded. In contrast to the sulfur system, the butterfly-shaped, classical isomer **3b** (natural charges, +0.584 bridgehead, +0.416 bridge, bo 1.255 and 1.173) is very close in energy to the rectangle **4b**, just 9 kJ/mol less stable (or 115 kJ/mol vs **5b**). The respective $4p^2 \rightarrow 4\sigma^*$ bonding in **3b** stabilizes the system by 76 kJ/mol and transfers in total about 0.20 electron into the $4\sigma^*$ orbitals. The least favorable isomer is **7b** (natural charges ranging from +0.398 to +0.585), 334 kJ/mol less stable than the global minimum **5b**.

First Ionization Potential of S_4 . In the course of this investigation, we found inconsistencies between the published, calculated and experimentally determined adiabatic first ionization potential of neutral S_4 ($IP_{\text{exptl}} = 989 \pm 29$ kJ/mol).^{27,29} We reassessed this property using the B3PW91/6-311+G(3df)//B3PW91/6-311+G* level of theory, and summarize the results here together with Niessens's^{27a} and Quelch's^{27b} earlier findings at the CI level with large basis sets. All earlier theoretical calculations agree on a D_{4h} symmetric square as the global minimum on the S_4^+ hypersurface.^{27a,39} Using the reported C_{2v} geometry of neutral S_4 ,²⁸ Niessen et al.^{27a} found a relaxed adiabatic first ionization potential of 776 kJ/mol. Similarly we find a relaxed adiabatic ionization potential of 826 kJ/mol employing the B3PW91/6-311+G(3df)//B3PW91/6-311+G* level of theory.⁴⁰ The vertical ionization potential of S_4 (C_{2v}) at the given level is 845 kJ/mol, still 144 kJ/mol from the experimental value but in agreement with the findings of Quelch et al. (839 kJ/mol).^{27c} Therefore, it is very likely that the experimentally determined adiabatic ionization potential of S_4 is not the ionization potential of the C_{2v} symmetric neutral tetrasulfur. In the experiment, sulfur or a metal sulfide MS ($M = Cd, Hg, Ag_2$) is heated between 500 and 1200 K, and the resulting sulfur vapor is analyzed.⁴¹⁻⁴³ All published determinations of the ionization potentials of neutral S_n ($n = 2-8$) agree on very low intensities of the observed S_4^+ ion. This complicates accurate threshold determination of the ionization process, but is explained by a comparison of the gaseous experimental heats of formation of neutral S_n in Table 4.²⁹

(39) Rhagavachari, K.; McMichael Rohlfling, C.; Binkley, J. S. *J. Chem. Phys.* **1990**, *93*, 5862.

(40) S_4^+ (D_{4h} symmetry), optimized parameter at the B3PW91/6-311+G* level of theory: $d(S-S) = 2.096$ Å, true minimum, $N_{\text{imag}} = 0$.

(41) Berkowitz, J.; Marquart, J. R. *J. Chem. Phys.* **1963**, *39*, 275.

(42) Berkowitz, J.; Lifshitz, C. *J. Chem. Phys.* **1968**, *48*, 4346.

(43) Rosinger, W.; Grade, M.; Hirschwald, W. *Ber. Bunsen-Ges. Phys. Chem.* **1983**, *87*, 536 and references therein.

S_4 has the highest experimental heat of formation of all S_n ($n = 2-7$) molecules, and S_6 has the lowest; thus, S_6 has the highest intensities in the mass spectrum (apart from S_8). In a photoionization study of these sulfur vapors, J. Berkowitz⁴² clearly demonstrated that the appearance potential of S_4^+ of about 10.4 ± 0.3 eV ($=1003 \pm 29$ kJ/mol) is *not* due to ionization of the parent neutral S_4 but that formed in a fragmentation process, i.e.



The same holds for the homologous selenium system (Se_4^+ is a fragment ion).⁴⁴ A later electron impact study,⁴³ which found an appearance potential of 10.1 ± 0.3 eV (975 ± 29 kJ/mol) did not show that the detected S_4^+ ion was not formed by fragmentation. Therefore, it is very likely that the (averaged) appearance potential of both determinations (10.25 ± 0.3 eV $= 989 \pm 29$ kJ/mol) resembles the threshold determination of the fragmentation reaction of neutral S_6 to give S_4^+ and S_2 , in fact ΔH_f for eq 1. To prove this, we fully optimized neutral S_6 in D_{3d} symmetry at the B3PW91/6-311+G* level of theory.^{45,46} At the B3PW91/6-311+G(3df)//B3PW91/6-311+G* level of theory, the heat of reaction for the fragmentation of neutral S_6 to give S_4^+ and triplet S_2 is 995 kJ/mol (or 10.31 eV), which is very near the averaged experimental value of 989 kJ/mol (or 10.25 eV). Taking this heat of reaction and the known heats of formation of neutral S_6 (102 kJ/mol) and S_2 (129 kJ/mol),²⁹ one can thus calculate the heat of formation of gaseous S_4^+ , i.e.

$$\Delta H_f(S_4^+_{(g)}, 298 \text{ K}) = \Delta H_f(S_{6(g)}, 298 \text{ K}) + \Delta H_f(\text{eq 1}) - \Delta H_f(S_{2(g)}, 298 \text{ K})$$

$$\Delta H_f(S_4^+_{(g)}, 298 \text{ K}) = ((102 \pm 8) + 995 - (129 \pm 1)) = 968 \pm 9 \text{ kJ/mol}$$

Using the experimental threshold value of 989 kJ/mol, a heat of formation of 962 kJ/mol is derived, both very different from the published value for $\Delta H_f(S_4^+_{(g)})$ of 1131 kJ/mol.²⁹ An ionization potential of S_4 of 822 ± 17 kJ/mol is obtained by subtracting the experimental enthalpy of formation of neutral S_4 (146 ± 8 kJ/mol)²⁹ from $\Delta H_f(S_4^+_{(g)})$ (968 ± 9 kJ/mol). This is in excellent agreement with our calculation of 826 kJ/mol (B3PW91/6-311+G(3df)//B3PW91/6-311+G*). Therefore, the true, relaxed adiabatic ionization potential of C_{2v} symmetric neutral tetrasulfur is 826 kJ/mol (calcd). Adding the experimental heat of formation of gaseous S_4 (146 ± 8 kJ/mol) leads to the heat of formation of gaseous square planar S_4^+ as:

$$\Delta H_f(S_4^+_{(g)}, 298 \text{ K}) = \Delta H_f(S_{4(g)}, 298 \text{ K}) + \text{first IP} \quad (S_{4(g)}, 298 \text{ K})$$

$$\Delta H_f(S_4^+_{(g)}, 298 \text{ K}) = ((146 \pm 8) + 826) = 972 \pm 8 \text{ kJ/mol}$$

This heat of formation is in excellent agreement with the above independently derived value of 968 kJ/mol and is close to the experimentally determined values for S_5^+ (939 kJ/mol), S_6^+ (971

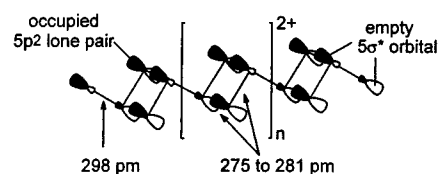


Figure 6. Charge delocalization by a $5p^2 \rightarrow 5\sigma^*$ interaction in polymeric, Zintl precise $(Te_4^{2+})_n^{2-}$

kJ/mol), and S_7^+ (951 kJ/mol), but lower than those found for S_2^+ and S_3^+ (1031 and 1076 kJ/mol, respectively).²⁹ The differences are smaller for the pure ionization potentials (see Table 4), reflecting the decreasing heats of formation (per sulfur atom) of the larger neutral molecules. Neutral S_4 with a square planar geometry would have four $3p_z$ lone pairs perpendicular to the plane of the ring and thus be very strained, in fact so strained that the ring opens up to give the planar C_{2v} ground state.²⁷ The highest occupied orbital of S_4 is therefore at high energy, reflecting the high ring strain, and the first ionization energy is therefore understandably low. In general, the more strained the ring, the lower the ionization energy. Since the unpaired electron in the square planar S_4^+ cation is found in a π^* orbital (see above, bonding in S_4^{2+}), the positive charge in this species is spread evenly over all sulfur atoms (average charge +0.25), and half a π bond is gained [cf. calculated $d(S-S)$ in S_4^+ , 2.096 Å; in S_4^{2+} with one π bond, 2.053 Å (B3PW91/6-311+G*)]. Additionally, the unpaired electron is delocalized over four rather than two or three atoms (cf. the higher ionization potentials of S_2 and S_3).

Bonding in Dimeric $(Te_4^{2+})_2$ and Polymeric $(Te_4^{2+})_n$. To analyze the bonding in the tellurium species, we optimized the M_4^{2+} geometries **3**, **4**, and **5** also for Te_4^{2+} . However, for tellurium atoms only the 3-21G* basis set is included within Gaussian 94,⁴⁷ and therefore relative energies are not as accurate as those derived for S_4^{2+} and Se_4^{2+} . The square planar Te_4^{2+} dication is the most favored species as is the case for sulfur and selenium above. The highly π -bonded $(Te_2^+)_2$ **4** is not a minimum and collapses to the square. The butterfly analogue **3**⁴⁸ is only 86 kJ/mol higher in energy than the square **5**,⁴⁹ a smaller value than for the $M = S$ and Se cases. This implies that the classically, all- σ -bonded species is relatively more favored for the heavier tellurium M_4^{2+} dications. Polymerization of this butterfly-shaped Te_4^{2+} leads to the recently observed polymeric Te_4^{2+} structure (see Figure 1). $np^2 \rightarrow no^*$ bonding (Figure 5) is also envisaged to serve as a means to delocalize the positive charge in this classical, Zintl precise M_4^{2+} isomer. A graphic representation of this process is given in Figure 6.

The $5p^2 \rightarrow 5\sigma^*$ bonding model accounts for the experimentally observed bond lengths. The bond connecting the four-membered rings is rather long (2.98 Å) due to the presence of electron density in the antibonding $5\sigma^*$ orbital while the ring distances are in the range of normal Te-Te single bonds.

The structure of Te_8^{4+} (see Figures 7 and 8) is formally obtained by a dimerization of 2 equiv of the butterfly Te_4^{2+} **3**.

(47) Apart from pseudopotentials, which gave Te-Te bond lengths very different from experimental findings in salts of square planar Te_4^{2+} (tested: LanL2DZ, SDD, cep121).

(48) Optimization at the B3PW91/3-21G* level of theory (C_{2v}) led to a true minimum with a transannular Te-Te distance of 2.739 Å and a ring distance of 2.813 Å. The folding angle of the two three-membered rings reaches 90.1°. This geometry is 86 kJ/mol less favorable than the square planar species.

(49) Optimization at the B3PW91/3-21G* level of theory (D_{4h}) led to a true minimum with a Te-Te distance of 2.717 Å which compares reasonably well with the experimentally observed values of 2.67-2.68 Å (not corrected for librational motion, which will add approximately 1-2 pm).

(44) Berkowitz, J.; Chupka, W. A. *J. Chem. Phys.* **1966**, *45*, 4289.

(45) S_6 is the global minimum on the S_6 hypersurface and found in the solid state. S_6 (D_{3d} symmetry), optimized parameters at the B3PW91/6-311+G* level of theory: $d(S-S) = 2.098$ Å, $\angle(S-S-S) = 103.0^\circ$, $\angle(S-S-S-S) = 73.2^\circ$ [compare to solid S_6 (exptl), 2.057 Å, 102.6°, and 73.8° (not corrected for librational motion, which will add approximately 1 pm)], true minimum, $N_{\text{imag}} = 0$; calculations include the ZPE and are corrected to 298 K.

(46) Caron, A.; Donahue, J. *Acta. Crystallogr.* **1965**, *18*, 562.

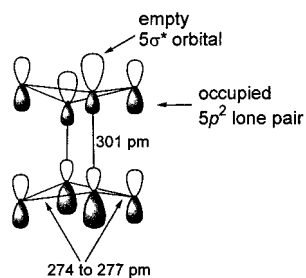


Figure 7. Bonding in Te_8^{4+} : intramolecular $5p^2 \rightarrow 5\sigma^*$ interactions.

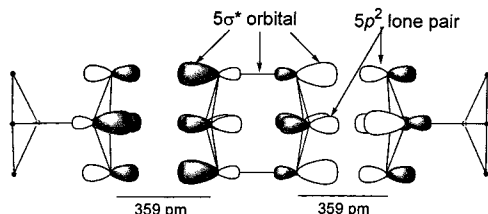


Figure 8. Bonding in Te_8^{4+} : intermolecular $5p^2 \rightarrow 5\sigma^*$ interactions.

The Te_8^{4+} units are weakly associated with an endless linear chain in the solid state.² The long Te–Te bonds connecting the two four-membered rings (3.01 Å) suggest the presence of electron density in the respective antibonding σ^* orbitals. The Te–Te bonds in the ring are in the range of normal Te–Te single bonds (2.74–2.77 Å). The Te_8^{4+} units in the endless chains are separated by 3.59 Å and are aligned along a 4-fold screw axis (see Figure 8). All these observations can be understood assuming a $5p^2 \rightarrow 5\sigma^*$ interaction as in Figure 5, allowing the unfavorable localized positive charges formally residing on the four tricoordinated Te atoms to be delocalized, as shown in Figures 7 and 8.

The occupied $5p^2$ lone pairs of the four dicoordinated Te atoms of the Te_4 rings donate electron density into the empty $5\sigma^*$ orbital of the two $\text{Te}^+ - \text{Te}^+$ bonds connecting the two four-membered rings. This interaction lengthens the two central Te–Te bonds (cf. 3.01 Å) and serves to delocalize the positive formal charges residing on the four tricoordinated atoms onto all eight atoms. Moreover, this model allows the formation of intermolecular interactions between the Te_8^{4+} units, every second of which is canted by 90° toward the others. In this orientation, an intermolecular $5p^2 - 5\sigma^*$ donor–acceptor interaction is favorable, which accounts for the short intermolecular distance of 3.59 Å and the chain-like arrangement of the cations in the solid state.

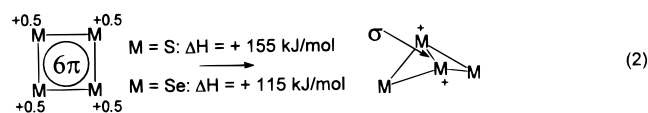
We note that the polymeric $(\text{Te}_4^{2+})_n$ and Te_8^{4+} cations are formed in the presence of the more basic, polymeric $(\text{VOCl}_4^{2-})_n$ (Te_8^{4+}) and a $\text{Bi}_2\text{Cl}_8^{2-}$ [$(\text{Te}_4^{2+})_n$] dianion, which is in contrast to the univalent counteranions of the square planar structures.^{1,2} This suggests that square planar Te_4^{2+} is preferred in the gas phase and in a nearly ideally ionic environment. The alternative polymeric structures are likely obtained as a consequence of some reduction of charge on the tellurium cation by anion–cation interactions, $5p^2 \rightarrow 5\sigma^*$ interactions, and the linear chainlike arrangement of the counterion.

Concluding Remarks

B3PW91 is an economical level of theory that gives accurate energies and geometries of sulfur and selenium M_4^{2+} cations, especially in combination with the 6-311G(2df) basis set. Reliable energies are computed at the B3PW91/6-311+G(3df)//B3PW91/6-311+G* level of theory. Employing the better B3PW91/6-311G(2df) geometries did not change the energies

relative to those obtained with the 6-311+G* geometries by more than a few kilojoules per mol. However, the inclusion of polarizing f functions is crucial in the energetic description of these strongly delocalized ions. The dependence on the basis set is much less pronounced in the selenium case, presumably due to less electrostatic repulsion in the larger dicationic system (e.g., from 2.0 to 2.3 Å widened interatomic separation).

Analysis of the examined seven sulfur (selenium) M_4^{2+} isomers reveals the presence of five (four) stationary points. In both systems the D_{4h} symmetric square planar geometries are the global minima, reflecting the experimentally observed solid-state structures. A rectangular D_{2h} structure is the next favorable isomer: 76 (Se, 106) kJ/mol less stable than the global minimum. A notable feature of the two structures lowest in energy (square and rectangle) is the unusual preference of $np_\pi - np_\pi$ bonds ($n = 3, 4$) over the classically formally σ -bonded butterfly structure **3** in which the charges are formally localized on adjacent chalcogen atoms. However, even in this structure positive charge is delocalized over all atoms by $np^2 \rightarrow n\sigma^*$ interactions. The energy of the selenium analogue **3b** is lowered as Se–Se distances are longer (e.g., the classical butterfly structure is only 9 kJ/mol less favorable than the D_{2h} rectangle, compared to 79 kJ/mol in the sulfur system). The tellurium butterfly analogue, which is a monomeric equivalent to Beck's polymeric, chain-like Te_4^{2+} (see Figure 1),² is even closer in energy to the square **4** [$E_{\text{rel}} = +86$ (Te) vs +115 (Se) and +155 (S) kJ/mol] while the $(\text{Te}_2^{2+})_2$ dimer **5** is not a minimum. Consistently different solid-state environments (anions) provide stabilization to at least three geometries of the average tellurium oxidation state +0.5 [square planar Te_4^{2+} , polymeric Te_8^{4+} , chain-like $(\text{Te}_4^{2+})_n$]. The latter two structures occur as salts of the rather basic dianions VOCl_4^{2-} and $\text{Bi}_2\text{Cl}_8^{2-}$ which have substantial anion–cation interaction via $np^2 \rightarrow n\sigma^*$ interactions, which reduce the positive charges residing on the dications and promote the adoption of the σ -bonded polymeric structures. However, for sulfur and selenium cations $np_\pi - np_\pi$ bonding ($n = 3, 4$) is preferred, and only the 6π -aromatic, square planar M_4^{2+} dication **5** is found experimentally. The delocalized π bond in **5** maximizes the positive charge delocalization and is more stable by 155 (115) kJ/mol than the formally σ -bonded species **3a** (**3b**) containing a σ bond between two tricoordinated formally unipositive chalcogen atoms (see eq 2).



This mirrors the situation in molecules containing group 14 and 15 $np_\pi - np_\pi$ bonds ($n \geq 3$) that are stabilized by the presence of bulky groups. Their respective alternative singly bonded oligomers are not formed because the resulting σ bonds are weakened due to steric hindrance.⁵⁰

This supports the thesis proposed by J.P.¹ to account for many of the unusual geometries of the homopolycationic cations of groups 16 and 17. Observed geometries of these cations and related species maximize positive charge delocalization, resulting in $np_\pi - np_\pi$ ($n \geq 3$), $\pi^* - \pi^*$ bonds, and bond length alternation.¹ We add to this proposal that the bond length alternation arises by $np^2 \rightarrow n\sigma^*$ interactions (Figure 5–8). These are more favored for tellurium relative to sulfur as the $np^2 - n\sigma^*$ energy difference is lower as the group is descended. $np^2 \rightarrow n\sigma^*$ bonding can be

(50) Burford, N.; Clyburne, J. A. C.; Chan, M. S. W. *Inorg. Chem.* **1997**, *36*, 3204.

viewed as responsible for the anion-cation interaction in salts of M_4^{2+} and in salts of mixed halogen-chalcogen cations, e.g., $[EX_3^+][MF_6^-]$ [E = S, Se, Te; X = F, Cl, Br, I (apart from SI_3^+); M = As, Sb],⁵¹⁻⁵⁴ which increases in strength as the group is descended.

Adding the derived gas-phase dimerization energy of $2S_2^+$ to give S_4^{2+} of 258 ± 9 kJ/mol in suitable Born-Fajans-Haber cycles and estimating lattice energies of salts of S_2^+ and S_4^{2+} by Kapustinskii's, Bartlett's, or Jenkin's empirical equations reveals that it is not possible to stabilize salts of the disulfur radical cation in the solid state, even when very large,

hypothetical anion volumes/radii are used [$\Delta H_{\text{lattice}} \propto 1/(r_{\text{cation}} + r_{\text{anion}})$].⁴ This is in contrast to the prediction of a stable S_2^+ salt⁴ of a large anion based on the dimerization energy of 443 kJ/mol.¹⁷ This illustrates the value of obtaining good quality thermodynamic estimates as an effective guide to the syntheses of hitherto unknown and novel cations (and anions).

Acknowledgment. We thank the Natural Sciences and Engineering Research Council (NSERC) of Canada (J.P., I.K.) and the Alexander von Humboldt Foundation in Bonn, Germany, for providing a Feodor-Lynen Fellowship (I.K.) and Dr. Holger Schwenk for the use of his RESVIEW program. We thank Dr. Friedrich Grein, University of New Brunswick (UNB), for many useful discussions and help in the course of this work as well as Isabelle Dionne, UNB, for lattice energy calculations which questioned the published dimerization energy. Jesus College, Oxford, is acknowledged with gratitude for a Senior Visiting Research Fellowship (1996-97, J.P.).

-
- (51) Johnson, J. P.; Murchie, M.; Passmore, J.; Tajik, M.; White, P. S.; Wong, C.-M. *Can. J. Chem.* **1987**, *65*, 2744.
(52) Christian, B. H.; Collins, M. J.; Gillespie, M. J.; Sawyer, M. J. *Inorg. Chem.* **1986**, *25*, 777.
(53) Brooks, W. V. F.; Passmore, J.; Richardson, E. K. *Can. J. Chem.* **1979**, *57*, 3230.
(54) Murchie, M. P.; Johnson, J. P.; Passmore, J.; Sutherland, G. W.; Tajik, M.; Whidden, T. K.; White, P. S.; Grein, F. *Inorg. Chem.*, **1992**, *31*, 274.

IC990048H